CELL STRUCTURE AND FUNCTION 39: 23–29 (2014)

Selection of an Aptamer against Mouse GP2 by SELEX

Misaho Hanazato[1,2], Gaku Nakato[1], Fumiko Nishikawa[3], Koji Hase[1,4], Satoshi Nishikawa[3], and Hiroshi Ohno[1,2]*

[1]*Laboratory for Intestinal Ecosystem, RCAI, RIKEN Center for Integrative Medical Sciences (IMS-RCAI), Kanagawa 230-0045,* [2]*Department of Supramolecular Biology, Graduate School of Nanobioscineces, Yokohama City University, Kanagawa 230-0045, Japan,* [3]*National Institute of Advanced Industrial Science and Technology, Tsukuba, Ibaraki 305-8566, Japan,* [4]*International Research and Development Center for Mucosal Vaccines, The Institute of Medical Science, The University of Tokyo, Tokyo 108-8639, Japan*

ABSTRACT. **Microfold (M) cells are intestinal epithelial cells specialized for sampling and transport of luminal antigens to gut-associated lymphoid tissue for initiation of both mucosal and systemic immune responses. Therefore, M-cell targeted vaccination has the potential to be a better immunization strategy. Glycoprotein 2 (GP2), an antigen uptake receptor for FimH$^+$ bacteria on M cells, can be a good target for this purpose. Aptamers are oligonucleotides that bind to a variety of target molecules with high specificity and affinity. Together with its low toxic feature, aptamers serves as a tool of molecular-targeted delivery. In this study, we used Systematic Evolution of Ligands by EXponential enrichment (SELEX) to isolate aptamers specific to murine GP2 (mGP2). After ten rounds of SELEX, eleven different aptamer sequences were selected. Among them, the most frequently appeared sequence (~60%) were aptamer NO. 1 (Apt1), and the second most (~7%) were aptamer NO. 5 (Apt5).** ***In vitro*** **binding experiment confirmed that only Apt1 and Apt5 specifically bound to mGP2 among eleven aptamers initially selected. Apt1 showed the strongest affinity with mGP2, with the Kd value of 110±2.6 nM evaluated by BIACORE. Binding assays with mutants of Apt1 suggest that, in addition to the loop structure, the nucleotide sequence, AAAUA, in the loop is important for binding to mGP2. Furthermore, this aptamer was able to bind to mGP2 expressed on the cell surface. These results suggest that this mGP2-specific aptamer could serve as a valuable tool for testing M-cell-targeted vaccine delivery in the murine model system.**

Key words: M cells, GP2, SELEX, aptamer

Introduction

Epithelial cells of the gastrointestinal tract are constantly exposed to a vast assortment of commensal bacteria and occasionally to pathogenic microorganisms. To protect themselves, the hosts have evolved gut-associated lymphoid tissue (GALT) such as Peyer's patches (PPs) and isolated lymphoid follicles (Miller *et al.*, 2007). GALT plays a critical role in recognition and uptake of intestinal antigens and induction of mucosal immune responses. The initial step of antigen-specific immune responses in GALT is sampling and transport of luminal antigens across the epithelial cells. Lymphoid follicles of GALT are covered by specialized epithelial cells called follicle-associated epithelium (FAE). Because the mucus barrier over the FAE is less than that over the villus epithelium, luminal antigens have relatively easy access to the cell surface of FAE. Microfold cells (M cells) are specialized epithelial cells located in FAE and are important for uptake and transport of luminal antigens to the immune cells of GALT (Bockman and Cooper, 1973; Owen, 1977). Unlike the absorptive enterocytes, M cells have a reduced glycocalyx and lack hydrolytic enzymes. Furthermore, the basal plasma membrane of M cells is deeply invaginated to form a pocket-like structure termed the 'M cell pocket', where dendritic cells (DCs) and lymphocytes are embraced. Owing to these characteristics, M cells can quickly transfer luminal antigens to antigen-presenting cells to induce antigen-specific antibody

*To whom correspondence should be addressed: Hiroshi Ohno, Laboratory for Intestinal Ecosystem, RCAI, RIKEN Center for Integrative Medical Sciences (IMS-RCAI), 1-7-22 Suehiro, Tsurumi, Kanagawa 230-0045, Japan.
Tel: +81–45–503–7031, Fax: +81–45–503–7068
E-mail: ohno@rcai.riken.jp

Abbreviations: GALT, gut-associated lymphoid tissue; PPs, Peyer's patches; FAE, follicle associated epithelium; M cells, microfold cells; GPI, glycosylphosphatidylinositol; GP2, glycoprotein 2; DCs, dendritic cells; m, murine; h, human; SELEX, Systematic Evolution of Ligands by EXponential enrichment.

responses, both mucosal IgA and systemic IgG (Nochi *et al.*, 2007). Based on the fact that antigen delivery thorough M cells is important for induction of efficient mucosal immune responses, M-cell targeted vaccines can be an effective strategy for mucosal immunization (Takahashi *et al.*, 2009).

We have reported that Glycoprotein 2 (GP2), a glycosylphosphatidylinositol (GPI) anchored protein, is exclusively expressed on the apical plasma membrane of M cells (Terahara *et al.*, 2008; Hase *et al.*, 2009). GP2 serves as an uptake receptor for type-I-piliated bacteria such as *Escherichia coli* and *Salmonella enterica* serovar Typhimurim to induce antigen-specific mucosal IgA response and systematic IgG responses to these bacteria (Hase *et al.*, 2009). These observations suggest that a good immunization strategy might be to develop a mucosal vaccine that targets GP2.

Antibodies and aptamers are among the best vehicles used for delivering molecules to specific targets. Aptamers are oligonucleotides that can bind to various targets such as small molecules, peptides and proteins with a high affinity and specificity (Hesselberth *et al.*, 2000). Compared to antibodies, aptamers possess distinctive advantages as molecular targeting vehicles: a relatively high binding affinity for various types of molecules, low-immunogenicity, and ease of synthesis and modification. In addition, aptamers are small enough to have a high renal clearance (Que-Gewirth and Sullenger, 2007). Owing to these advantages, aptamers may represent a valid alternative to antibodies, particularly for drug delivery (Bunka and Stockley, 2006).

In an attempt to obtain GP2-targeting vehicles for the development of an efficient mucosal vaccine delivery system, we employed an *in vitro* evolution process, Systematic Evolution of Ligands by EXponential enrichment (SELEX) (Ellington and Szostak, 1990; Tuerk and Gold, 1990), to screen RNA aptamers specific for murine GP2 (mGP2). Here, we report the isolation of a mGP2 specific aptamer with a Kd value of 110±2.6 nM and have determined the nucleotide sequences important for its binding to mGP2.

Materials and Methods

Recombinant protein preparation

Human embryonic kidney HEK293T cells were transfected with an mGP2-human IgG1 Fc fusion protein (mGP2-Fc) expression vector or a control human IgG1 Fc (Fc) expression vector (Hase *et al.*, 2009) and cultured for 7 days. The proteins (mGP2-Fc or Fc) secreted into the culture supernatant were purified with a HiTrap Protein A HP affinity column (GE Healthcare).

In vitro selection of RNA aptamer

The RNA library for *in vitro* selection consisted of a 30-nuculeotide random region (N30) flanked by two constant regions, 5'-GGGAGAAUUCCGACCAGAAG-(N30)-CCUUUCCUCUCUCCUUCCUCUUCU-3' (Kikuchi *et al.*, 2003). RNAs were denatured at 94°C for 2 min, and then cooled to room temperature in phosphate buffered saline (PBS). The RNA pool was mixed with mGP2-Fc and incubated in PBS at room temperature. After the incubation, the mixture was passed through a 0.45 μm HAWP nitrocellulose filter (Millipore) and washed with PBS. The mGP2-Fc-bound RNAs on the filter were recovered with 400 μl of 7 M urea at 90°C for 5 min. The eluted RNAs were ethanol precipitated and reverse transcribed using AMV reverse transcriptase (Roche Applied Science) at 42°C for 1 hour. The products were PCR amplified (94°C for 30 sec, 55°C for 30 sec and 72°C for 30 sec) using Gene Taq (Nippon Gene) with forward primer 5'-AGTAATACGACTCACTATAGGGAGAATTCCGACCAGAAG-3' and reverse primer, 5'-AGAAGAGGAAGGAGAGAGGAAAGG-3' (Invitrogen), and transcribed using the T7 Ampliscribe kit (Epicentre Technology). The RNA products were treated with DNase I and purified by Micro Bio-Spin Columns P-30 (Bio-Rad laboratories) or 8% PAGE containing 7 M urea. At the fourth and seventh rounds, magnetic beads (Dynabeads M-450 Epoxy; Dynal Biotech) were used instead of the nitrocellulose membrane for protein fixation. Table I summarizes the conditions used in each round of the selection.

Table I. Selection conditions

Round	RNA pool (μM)	mGP2 (μM)	tRNA (μM)	Time (min)	wash (μl×times)
1	10	1.0	0	60	500×1
2	5	0.5	5	30	500×1
3	2.5	0.25	15	20	500×2
4	2.5	0.15	30	15	500×3
5	1.25	0.1	60	10	500×4
6	1.25	0.05	120	10	500×5
7	1.25	0.05	120	10	500×6
8	1.25	0.05	120	10	500×7
9	1.25	0.05	120	10	500×8
10	1.25	0.05	120	10	500×9

Sequence analysis

After the tenth round of selection, the cDNA pool was inserted into the pGEM-T Easy vector (Promega) and cloned in *Escherichia coli* DH-5α strain (TOYOBO). Plasmid DNA was isolated using PureYield™ Plasmid Miniprep System (Promega) and the clones were sequenced with a 3130 Genetic Analyzer (Applied Biosystems).

Binding analysis of radiolabeled aptamers

The isolated aptamers and their mutants were radiolabeled by *in vitro* transcription as described above in the presence of [α^{32}P]ATP (PerkinElmer). The labeled aptamers were mixed with mGP2-Fc or Fc in PBS and incubated for 10 min at room temperature. The mixture was then filtered using HAWP nitrocellulose filter. Radio-

activity retained on the filter was counted with a BAS2000 Bioimaging Analyzer (Fuji Film). The binding activity was evaluated as the ratio of the radioactivity retained on the filter to that of total input.

Kinetic analysis of the binding of mGP2-specific aptamer with mGP2-Fc

Kinetic analysis was performed with a BIACORE 3000 (GE Healthcare). Twenty-five nM biotinylated GP2-specific aptamer was immobilized on a streptavidin-coated sensor chip (GE healthcare). Various concentrations of mGP2-Fc (0–1000 nM) in PBS were injected at a flow rate of 20 µl/min for 4 min for the association phase, and the dissociation phase was monitored by injecting PBS for 4 min. The data were analyzed with the BIAevaluation program version 3.2 (GE healthcare). Kinetic parameters were determined by a simple model, A+B=AB and the data were fit with local fit of kinetic simultaneous Ka/Kd model.

Prediction of the secondary structure of the aptamers

The secondary structure of aptamers was predicted by using the UNA Fold software. (http://www.idtdna.com/UNAFold/Home/Index).

Preparation of mutant aptamers

The template single-stranded DNAs including complementary sequences or deleted sequences of the loop region were synthesized (OPERON). These DNAs were used for *in vitro* transcription as described above. The mutant sequences are shown in Fig. 3.

Binding of the mGP2-specific aptamer to mGP2-expessing HeLa cells

HeLa cells cultured in DMEM (Sigma) containing 10% heat-inactivated fetal bovine serum were transfected with an mGP2 cDNA in pcDNA3 plasmid on coverslips. After 48 hours, the coverslips were washed with ice-cold PBS and fixed with 4% (w/v) paraformaldehyde for 20 min. Coverslips were washed with ice-cold PBS and incubated with a mixture of FITC-labeled mGP2-specific aptamer (Hokkaido System Science) and rat anti-mGP2 mAb (2F11-C3) (MBL) at room temperature for 60 min. The sample was further incubated with Alexa Fluor 555-conjugated donkey anti-rat IgG (H+L) antibody (Invitrogen). After washing with PBS, the samples were mounted with VECTASHIELD Mounting Medium with DAPI (VECTOR LABORATORIES) and observed by fluorescent microscopy (OLYMPUS-BX51).

Statistical analysis

Quantitative data are presented as mean±SD. Differences between two groups were analyzed by the Student's *t* test (Fig. 1) and to analyze the differences among three groups by analysis of variance (One-Way ANOVA followed by Turkey's post hoc test.) (Fig. 4).

Results

In vitro selection of aptamers against mGP2

To obtain aptamers specific for mGP2, we performed SELEX, with increasing selection pressure (Table I), using an RNA pool consisting of approximately 10^{14} different molecules with 30 nt randomized sequences flanked by two constant regions in a 74-nt long RNA. We used magnetic-bead selection instead of nitrocellulose filters in the fourth and seventh rounds to exclude system-dependent aptamers, i.e. those having affinity for the nitrocellulose filter. After ten rounds of SELEX, eleven different aptamer sequences were selected (Table II). Among them, about 60% were aptamer NO. 1 (Apt 1) and 7% were aptamer NO. 5 (Apt 5). There was no consensus sequence between these two aptamers.

Binding of aptamers to mGP2

To confirm the specific binding of these aptamers to mGP2, we incubated mGP2-Fc or Fc, as a negative control, with radiolabeled aptamers. The two most frequently appearing aptamers, Apt1 and Apt5, specifically bound to mGP2-Fc but not to Fc (Fig. 1). By contrast, the other aptamers failed to specifically bind mGP2-Fc (Fig. 1).

Since Apt1 showed the highest binding ability for mGP2, we focused mainly on this aptamer for the rest of the study. The kinetic analysis with BIACORE showed that the binding of Apt1 to mGP2 increased in response to the increment of mGP2 concentration (Fig. 2). The K_d value evaluated by BIACORE of the binding kinetics of Apt1 with mGP2 was 110±2.6 nM.

Identification of the critical region in Apt1 for binding to mGP2

The loop region of aptamers is often important for binding

Table II. Sequences in the random region of selected aptamers

		(%)
Apt1	CAAGUAGUUGGCGCCUACUAUAGAAAUACG	(59.3)
Apt2	UGCUUUUGGUGGAGGUGGUAGCACUGGCGG	(3.7)
Apt3	CACGUUGGUGGUGGAGGUGUGCUGAGGUCC	(3.7)
Apt4	GAUGGCUCAAGUUGGUGGUGGUGGAUUGGG	(3.7)
Apt5	CGUACACGUUAGUUGAGAUUACCCCUGGUC	(7.4)
Apt6	CUCAUUGGUGGAGGUGGAGAGCUUUUGGUU	(3.7)
Apt7	GAUAGUGUCACGAUGGAGGUGGUGGUGUGA	(3.7)
Apt8	GGAUGAACGGCCUGUGGGGGGGGGAGGAGGC	(3.7)
Apt9	CGCGUAGGAGGUGGUGGAGCGUUUUUGGUC	(3.7)
Apt10	GCCUAUGGUGGAGGUGGAUGGCUGCUGCGU	(3.7)
Apt11	CGAUUGGGUGGUGGAGGUGCUUUGGGUCUC	(3.7)

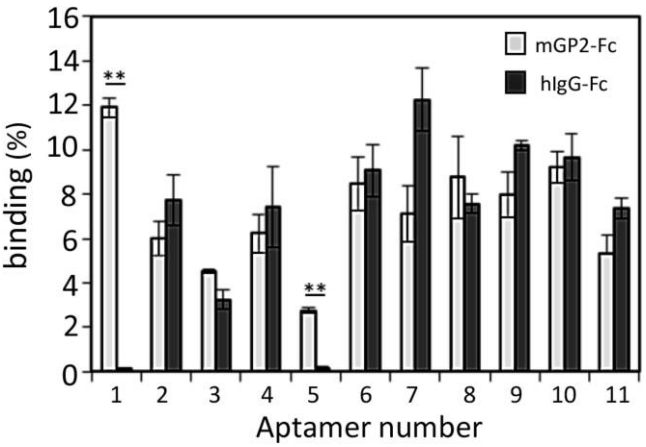

Fig. 1. Binding specificity of SELEX-selected aptamers for mGP2. The binding activity of ^{32}P-radiolabeled aptamers was measured as described in Materials and Methods. Binding is shown as the percentage of the radioactivity retained on the filter compared to that of the total input. Data are mean±SE values (n=3). **p<0.01.

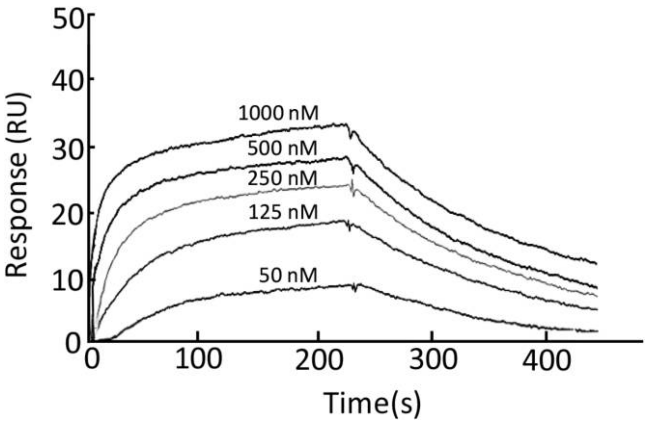

Fig. 2. Kinetic analysis of the Apt1 binding with mGP2. Kinetic analysis was performed with a BIACORE as described in Materials and Methods. Sensorgrams are shown for immobilized Apt1 interacting with various concentrations of mGP2-Fc.

to its target (Mi *et al.*, 2009). Therefore, we examined whether the loop region in Apt1 was involved in its binding to mGP2. We synthesized two mutants of Apt1, mD1 and mD2 which lack the predicted loop structures, loop 1 and loop 2, respectively (Fig. 3). Both mD1 and mD2 no longer bound to mGP2. We also constructed additional mutants, mC1 and mC2, in which the nucleotide sequence of loop 1 and loop 2 were replaced with their complementary sequences (Fig. 3). Although the predicted structure of these aptamers maintained the same loop structure as Apt1, both aptamers showed reduced binding to mGP2; 84% and 63% reduction for mC1 and mC2, respectively, compared to Apt1 (Fig. 3 and Fig. 4). These results suggest that loop1 is more important than loop 2 for the binding to mGP2 and that the nucleotide sequence of loop 1, AAAUA, in addition to its three-dimensional structure, contributes to the binding with mGP2.

Binding of Apt1 to mGP2-expressing HeLa cells

In order for the aptamers to act as a vehicle for drug/vaccine delivery, they have to bind to their target molecule in its naturally existing form. To examine this point, we tested the binding of Apt1 to HeLa cells transiently expressing mGP2 on the cell surface. As shown in Fig. 5, we were able to detect the colocalization of Apt1 and anti-mGP2 antibody, indicating that Apt1 can bind to mGP2 expressed on the cell surface.

Discussion

In this study, we have reported the isolation and characterization of an RNA aptamer that specifically binds to mGP2. We first obtained eleven aptamers by SELEX, using mGP2-Fc as the bait. Subsequent *in vitro* binding assays revealed that, among the selected aptamers, two of them, Apt1 and Apt5, were able to specifically bind to mGP2 (Fig. 1). We evaluated the kinetics of Apt1 since it had the highest affinity and specificity, and the K_d value for Apt1 was 110±2.6 nM, the strongest binder of mGP2-Fc. This is still relatively weak compared to the Kd value of 10^{-9}~10^{-11} M for aptamers reported previously (Keefe *et al.*, 2010).

In general, frequently selected aptamer sequences tend to possess a consensus sequence and/or share a similar structure (Kikuchi *et al.*, 2003; Vaish *et al.*, 2003). However, there was no consensus sequence between Apt1 and Apt5 in the random sequence region, suggesting that the secondary structure, rather than a consensus sequence, is important for the binding of these aptamers to mGP2. Therefore, we focused on the secondary structure. Their secondary structures were predicted using the UNA Fold program. Both aptamers likely conformed to a stem-loop structure in the randomized region, although their structures did not resemble each other (our unpublished observation).

Indeed, *in vitro* binding assays with Apt1 deletion mutants suggested that the loop1 region of Apt1 is important for its binding to mGP2 (Fig. 3). However, replacement of the 'AAAUA' sequence in the loop region with the complimentary sequence markedly reduce the binding affinity to mGP2, suggesting that this nucleotide sequence also contributes to the binding to mGP2 (Fig. 3 and Fig. 4).

We have also shown in this study that Apt 1 can bind to mGP2 expressed on the cell surface, which is prerequisite for any *in vivo* application of aptamers (Fig. 5). Our ultimate goal for the GP2-specific aptamer is its future application for the development of a GP2-targeted, efficient

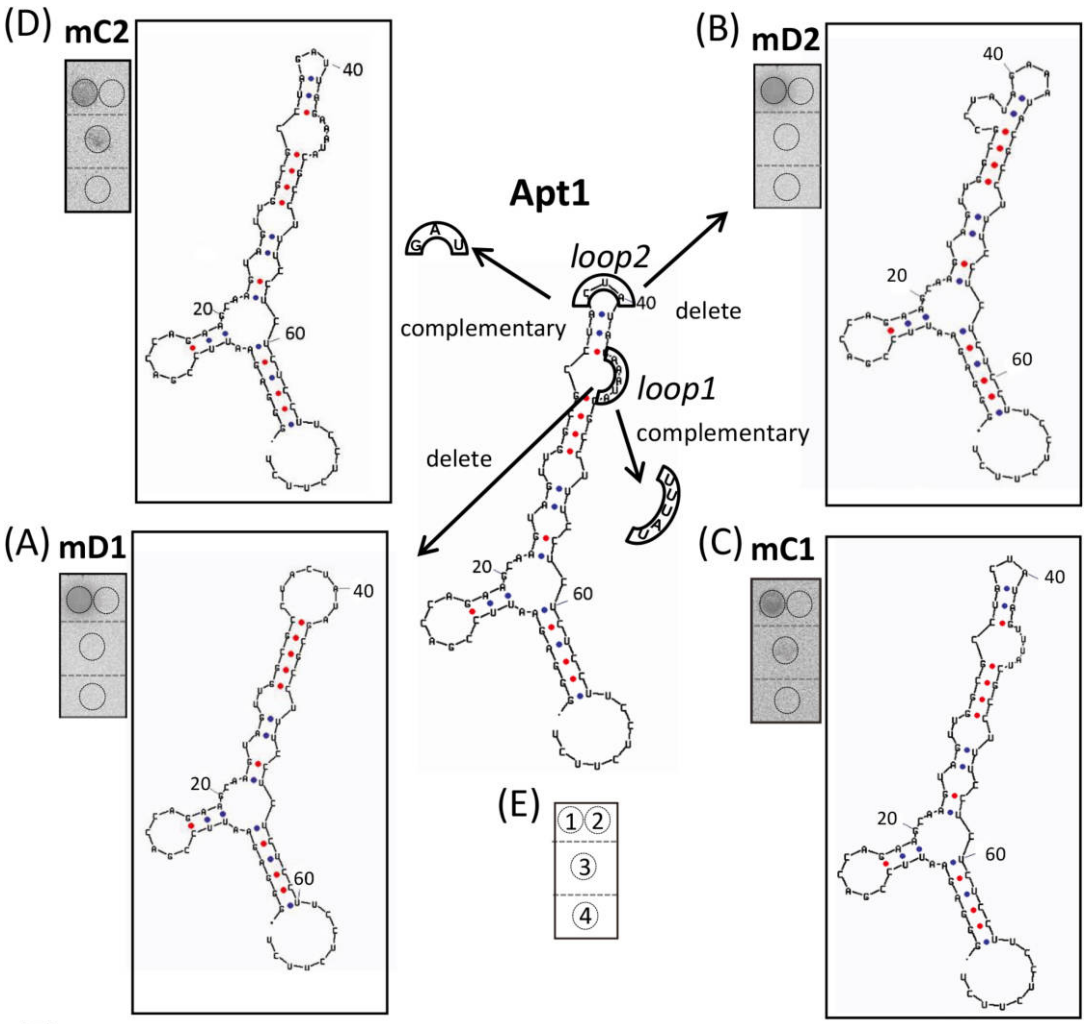

(F)

mutant sequences

mC1

5′-GGGAGAAUUCCGACCAGAAGCAAGUAGUUGGCGCCUACUAUAG***UUUAU***CGCCUUUCCUCUCUCCUUCCUCUUCU-3’

mC2

5′-GGGAGAAUUCCGACCAGAAGCAAGUAGUUGGCGCCUA***GAU***UAGAAAUACGCCUUUCCUCUCUCCUUCCUCUUCU-3’

mD1

5′-GGGAGAAUUCCGACCAGAAGCAAGUAGUUGGCGCCUACUAUAGCGCCUUUCCUCUCUCCUUCCUCUUCU-3’

mD2

5′-GGGAGAAUUCCGACCAGAAGCAAGUAGUUGGCGCCUAUAGAAAUACGCCUUUCCUCUCUCCUUCCUCUUCU-3’

Fig. 3. Predicted secondary structures and binding activity of Apt1 and its mutants. The secondary structure of aptamers was predicted by UNA Fold. (A, B) The structures of the loop-deleted aptamers. (C, D) The aptamers that have complementary sequences in their loop regions. The binding of these mutant aptamers with mGP2 is shown as dot blots (A–D). Positions of the plots are enclosed with circles. (E) Samples plotted at each position is as follows; 1, the total input of each mutant aptamer used for the binding assay (without washing). 2, aptamer alone (without addition of any proteins). 3, aptamer with mGP2-Fc. 4, aptamer with hIgG-Fc. (F) Sequence of mutant aptamers. 5' and 3' constant regions of aptamers are underlined. Italic bold letters indicate the sequences altered in the mutants.

mucosal vaccine delivery system. To this end, the obtained aptamer has to reach intestinal M cells via the oral route, which could present some technical challenges. Aptamers, especially RNA aptamers, are susceptible to degradation by nucleases. Furthermore, aptamers might be recognized by Toll-like receptors (TLRs) 3, 7, 8 and 9 and modulate immune responses (Akira *et al.*, 2006), although it has been suggested that TLR recognition of aptamers might actually be advantageous for vaccines since it could exert an adjuvant effect (Koyama *et al.*, 2009). Common strategies to overcome nuclease degradation are modification of the 2' position of the ribose ring by fluorination and methylation (Green *et al.*, 1995; Healy *et al.*, 2004) and incorporation of aptamers into liposomes (Willis *et al.*, 1998). The methylation modification has also been reported to reduce the risk of TLR recognition (Yu *et al.*, 2009). On the other hand, a major negative aspect of these modifications is that modified aptamers often lose ligand binding ability because of the resulting structural change. In fact, fluorinated Apt1 lost its mGP2-binding capacity in our hands (our unpublished observation).

Another possibility for delivering aptamers to M cells is changing the route of administration. Accumulating studies have reported that M cells exist not only in FAE of GALT but also in the nasopharynx-associated lymphoid tissue (NALT) (Spit *et al.*, 1989; Kiyono and Fukuyama, 2004). We have confirmed the expression of GP2 by NALT M cells (our unpublished observation). Considering the many

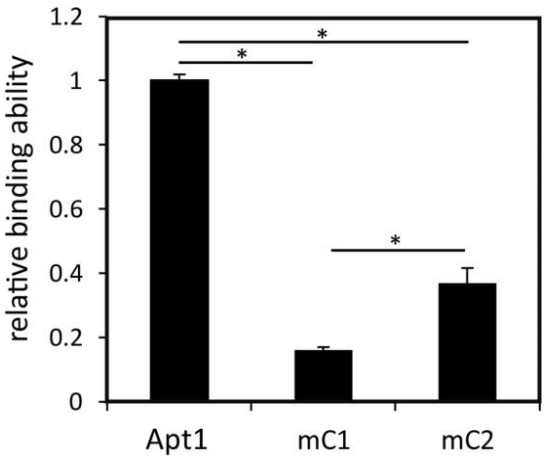

Fig. 4. Binding affinity of Apt1 mutants mC1 and mC2 with mGP2. The binding activity of ^{32}P-radiolabeled aptamers was measured as described in Materials and Methods. Results are shown as the relative radioactivity of the mutants bound to mGP2 compared to that of Apt1. Data are mean ±SE values (n=3). *p<0.05.

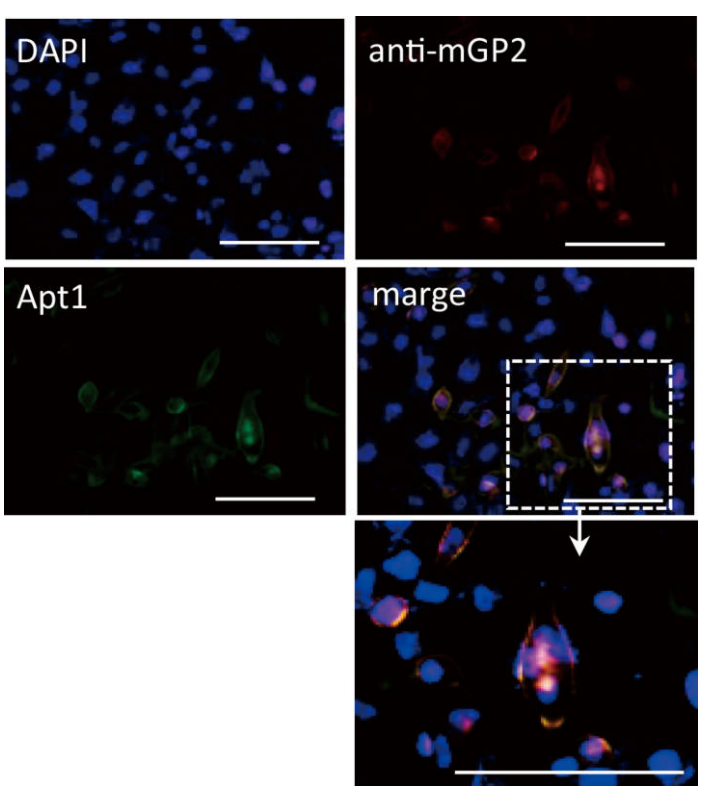

Fig. 5. Binding of Apt1 to cells expressing cell surface mGP2. HeLa cells transiently expressing mGP2 were incubated with FITC-labeled Apt1 (green) and anti-mGP2 mAb, followed by Alexa Fluor 555-conjugated secondary antibody to visualize mGP2 (red). Scale bars, 100 μm.

pathogens such as influenza virus that infect through the respiratory tract, NALT should be an important barrier against infection and for induction of mucosal immune responses (Kiyono and Fukuyama, 2004; Brandtzaeg, 2011). Since the delivery distance of aptamers to nasal M cells is far less than that of intestinal M cells, the risk of degradation should be decreased. In addition, human tonsils are known to resemble mouse NALT tissue (Perry and Whyte, 1998; Park *et al.*, 2003; Cesta, 2006). Therefore, the administration of GP2-specific aptamers through NALT is a promising protocol for mucosal vaccine delivery.

In conclusion, our mGP2-specific aptamer should be a useful tool for testing M-cell-targeted drug/vaccine delivery in the murine model system.

Acknowledgments. We would like to thank P. D. Burrows for critical reading of the manuscript and Y. Yamada for secretarial assistance. This study was supported in part by Grant-in-Aid for Research Activity Start-up (G.N.), Grants-in-Aid for Young Scientists (B) (G.N.), Grants-in-Aid for Young Scientists (A) (K.H.), Scientific Research (B) (H.O.) and Scientific Research (A) (H.O.) from the Japan Society for the Promotion of Science, Grant-in-aid for Scientific research on priority areas (K.H.) and Scientific Research on Innovative Areas (H.O.) from the Ministry of Education, Culture, Sports, Science and Technology of Japan, The Sasakawa scientific research grant from the Japan science society (G.N.), The Sumitomo Foundation (K.H.), The Uehara Memorial Foundation (K.H.) and The Mitsubishi Foundation (H.O.).

References

Akira, S., Uematsu, S., and Takeuchi, O. 2006. Pathogen recognition and innate immunity. *Cell*, **124**: 783–801.

Bockman, D.E. and Cooper, M.D. 1973. Pinocytosis by epithelium associated with lymphoid follicles in the bursa of Fabricius, appendix, and Peyer's patches. An electron microscopic study. *Am. J. Anat.*, **136**: 455–477.

Brandtzaeg, P. 2011. Potential of nasopharynx-associated lymphoid tissue for vaccine responses in the airways. *Am. J. Respir. Crit. Care. Med.*, **183**: 1595–1604.

Bunka, D.H. and Stockley, P.G. 2006. Aptamers come of age - at last. *Nat. Rev. Microbiol.*, **4**: 588–596.

Cesta, M.F. 2006. Normal structure, function, and histology of mucosa-associated lymphoid tissue. *Toxicol. Pathol.*, **34**: 599–608.

Ellington, A.D. and Szostak, J.W. 1990. *In vitro* selection of RNA molecules that bind specific ligands. *Nature*, **346**: 818–822.

Green, L.S., Jellinek, D., Bell, C., Beebe, L.A., Feistner, B.D., Gill, S.C., Jucker, F.M., and Janjic, N. 1995. Nuclease-resistant nucleic acid ligands to vascular permeability factor/vascular endothelial growth factor. *Chem. Biol.*, **2**: 683–695.

Hase, K., Kawano, K., Nochi, T., Pontes, G.S., Fukuda, S., Ebisawa, M., Kadokura, K., Tobe, T., Fujimura, Y., Kawano, S., Yabashi, A., Waguri, S., Nakato, G., Kimura, S., Murakami, T., Iimura, M., Hamura, K., Fukuoka, S., Lowe, A.W., Itoh, K., Kiyono, H., and Ohno, H. 2009. Uptake through glycoprotein 2 of FimH(+) bacteria by M cells initiates mucosal immune response. *Nature*, **462**: 226–230.

Healy, J.M., Lewis, S.D., Kurz, M., Boomer, R.M., Thompson, K.M., Wilson, C., and McCauley, T.G. 2004. Pharmacokinetics and biodistribution of novel aptamer compositions. *Pharm. Res.*, **21**: 2234–2246.

Hesselberth, J., Robertson, M.P., Jhaveri, S., and Ellington, A.D. 2000. *In vitro* selection of nucleic acids for diagnostic applications. *J. Biotechnol.*, **74**: 15–25.

Keefe, A.D., Pai, S., and Ellington, A. 2010. Aptamers as therapeutics. *Nat. Rev. Drug Discov.*, **9**: 537–550.

Kikuchi, K., Umehara, T., Fukuda, K., Hwang, J., Kuno, A., Hasegawa, T., and Nishikawa, S. 2003. RNA aptamers targeted to domain II of hepatitis C virus IRES that bind to its apical loop region. *J. Biochem.*, **133**: 263–270.

Kiyono, H. and Fukuyama, S. 2004. NALT- versus Peyer's-patch-mediated mucosal immunity. *Nat. Rev. Immunol.*, **4**: 699–710.

Koyama, S., Coban, C., Aoshi, T., Horii, T., Akira, S., and Ishii, K.J. 2009. Innate immune control of nucleic acid-based vaccine immunogenicity. *Expert. Rev. Vaccines.*, **8**: 1099–1107.

Mi, Z., Guo, H., Russell, M.B., Liu, Y., Sullenger, B.A., and Kuo, P.C. 2009. RNA aptamer blockade of osteopontin inhibits growth and metastasis of MDA-MB231 breast cancer cells. *Mol. Ther.*, **17**: 153–161.

Miller, H., Zhang, J., Kuolee, R., Patel, G.B., and Chen, W. 2007. Intestinal M cells: the fallible sentinels? *World J. Gastroenterol.*, **13**: 1477–1486.

Nochi, T., Yuki, Y., Matsumura, A., Mejima, M., Terahara, K., Kim, D.Y., Fukuyama, S., Iwatsuki-Horimoto, K., Kawaoka, Y., Kohda, T., Kozaki, S., Igarashi, O., and Kiyono, H. 2007. A novel M cell-specific carbohydrate-targeted mucosal vaccine effectively induces antigen-specific immune responses. *J. Exp. Med.*, **204**: 2789–2796.

Owen, R.L. 1977. Sequential uptake of horseradish peroxidase by lymphoid follicle epithelium of Peyer's patches in the normal unobstructed mouse intestine: an ultrastructural study. *Gastroenterology*, **72**: 440–451.

Park, H.S., Francis, K.P., Yu, J., and Cleary, P.P. 2003. Membranous cells in nasal-associated lymphoid tissue: a portal of entry for the respiratory mucosal pathogen group A streptococcus. *J. Immunol.*, **171**: 2532–2537.

Perry, M. and Whyte, A. 1998. Immunology of the tonsils. *Immunol. Today*, **19**: 414–421.

Que-Gewirth, N.S. and Sullenger, B.A. 2007. Gene therapy progress and prospects: RNA aptamers. *Gene Ther.*, **14**: 283–291.

Spit, B.J., Hendriksen, E.G., Bruijntjes, J.P., and Kuper, C.F. 1989. Nasal lymphoid tissue in the rat. *Cell Tissue Res.*, **255**: 193–198.

Takahashi, I., Nochi, T., Yuki, Y., and Kiyono, H. 2009. New horizon of mucosal immunity and vaccines. *Curr. Opin. Immunol.*, **21**: 352–358.

Terahara, K., Yoshida, M., Igarashi, O., Nochi, T., Pontes, G.S., Hase, K., Ohno, H., Kurokawa, S., Mejima, M., Takayama, N., Yuki, Y., Lowe, A.W., and Kiyono, H. 2008. Comprehensive gene expression profiling of Peyer's patch M cells, villous M-like cells, and intestinal epithelial cells. *J. Immunol.*, **180**: 7840–7846.

Tuerk, C. and Gold, L. 1990. Systematic evolution of ligands by exponential enrichment: RNA ligands to bacteriophage T4 DNA polymerase. *Science*, **249**: 505–510.

Vaish, N.K., Larralde, R., Fraley, A.W., Szostak, J.W., and McLaughlin, L.W. 2003. A novel, modification-dependent ATP-binding aptamer selected from an RNA library incorporating a cationic functionality. *Biochemistry*, **42**: 8842–8851.

Willis, M.C., Collins, B.D., Zhang, T., Green, L.S., Sebesta, D.P., Bell, C., Kellogg, E., Gill, S.C., Magallanez, A., Knauer, S., Bendele, R.A., Gill, P.S., and Janjić, N. 1998. Liposome-anchored vascular endothelial growth factor aptamers. *Bioconjug. Chem.*, **9**: 573–582.

Yu, D., Wang, D., Zhu, F.G., Bhagat, L., Dai, M., Kandimalla, E.R., and Agrawal, S. 2009. Modifications incorporated in CpG motifs of oligodeoxynucleotides lead to antagonist activity of toll-like receptors 7 and 9. *J. Med. Chem.*, **52**: 5108–5114.

(Received for publication, September 2, 2013, accepted, December 2, 2013 and published online, December 12, 2013)